Strojniški vestnik - Journal of Mechanical Engineering vol(yyyy)no, p-p
DOI code
Original / Review / Short Scientific Paper
Received for review: yyyy-mm-dd
Received revised form: yyyy-mm-dd
Accepted for publication: yyyy-mm-dd
© 2015 Journal of Mechanical Engineering. All rights reserved.

Preliminary Comparison of the Performance Thermodynamic Models of the Subsonic Ejector and Turbofan

Vytautas Martinaitis[1] – Dovydas Rimdžius[1] – Juozas Bielskus[1] – Giedrė Streckienė[1,*] – Violeta Motuzienė[1]
[1] Vilnius Gediminas Technical University, Department of Building Energetics, Lithuania

Flow-mixing is common in technological processes and both ejectors and turbofans are able to realize the interaction between flows with different energy potentials. Ejectors have been extensively used and their analytical models have been widely presented. Meanwhile to the best of authors' knowledge there is a lack of studies exploring efficiencies of turbofans. The goal of this paper is to compare thermodynamic processes in these devices. Their efficiencies are compared in terms of compression and entrainment ratios. A comprehensive one-dimensional subsonic thermodynamic models of the ejector and turbofan are presented. The quantitative indices are obtained for the same initial conditions expressed as the ratio of differences in enthalpies for ideal compression and ideal expansion. When initial conditions are equal to the numeric value of the combination of isentropic efficiency of evaluated components (numerical case 0.16), both devices have the same efficiencies; at lower initial conditions (numerical case 0.10), turbofan's entrainment ratio is 1.5 times and compression efficiency 1.25 times higher; at higher value of initial conditions (numerical case 0.28) – the ejector is more efficient. Such distinctive characteristics of turbofans and the nature of their variation may correspond to the specific application areas of the technological equipment, which require certain flow mixing parameters.

Keywords: ejector, turbofan, thermodynamic model, flow mixing, efficiency of compression, entrainment ratio

Highlights*:*

- Thermodynamic processes of gas mixing in the ejector and the turbofan are compared.
- The efficiency of compression and entrainment ratios are compared in subsonic mode.
- When entrainment ratios are low, the ejector is more advantageous than turbofan.
- Turbofan can be applied where a relatively higher passive flow rate is required.
- Isentropic efficiencies are highly dependent on features of each component.

0 INTRODUCTION

Flow-mixing processes are common in the devices of many technological systems. These processes are realized in components such as ducts, nozzles, diffusers, throttling valves, mixing chambers, turbines, compressors, ventilators. Mixing flows with different parameters in the mixing chamber are usually aimed at the increase of the efficiency and operational abilities of these devices. Presented analysis relates to different flow mixing devices in which the mixing of two gas flows takes place due to different energy potentials. Such cases are sketched in Fig. 1.

Ejector (Fig. 1 (a)) is a very well-known device, meanwhile roof turbine ventilator (b) has spread over the last decade worldwide as device using renewable wind energy for buildings' ventilation. Turbofans – gas mixers (c) are used rarely, although they have been known for a long time as gas burners' mixers. Despite similarities with other mentioned devices, turbofans – engines (d) will not be discussed further because of their complexity and significant difference in scope of operation compared to other above described mixers.

The roof turbine rotor (b) on the side from which the wind blows operates as turbine, and from the opposite side – as fan. Besides, ejection processes are happening in it. During operation of this device very complex processes occur, that could be a reason why to the best of the authors' knowledge until now there is no theoretical, thermodynamic model to describe operation of the roof turbine ventilator. In provided examples common is the interaction and mixing between flows that have varying energy potentials. The models of classical thermodynamic analysis enable to understand the operation of the technical system; to determine the places and

*Corr. Author's Address: Vilnius Gediminas Technical University, Department of Building Energetics, Saulėtekio ave. 11, Vilnius, Lithuania, giedre.streckiene@vgtu.lt

causes of irreversibility of energy conversion processes; to compare performance of the technical systems which are described in the same way.

This paper focuses on conceptual comparison of two above shown devices – ejector (a) and turbofan-gas mixer (c). The ejector will be used as baseline for such comparison, as the ejectors thermodynamic models have strong practical and scientific validation. The turbofan (c) has clearly separated turbine and fan, therefore their preliminary comparison requires less debatable assumptions (e.g. compared to the roof turbine ventilator (b), Fig. 1), has a close logical sequence same as ejector.

Nowadays, application of ejectors has spread to various thermal engineering facilities. Ejectors are used in various areas: vapor-compression refrigeration systems [1]; in buildings and vehicles ventilation [2], district heating [3], etc. However, recently the application and improvement of ejectors in refrigeration equipment has been at the center of most studies [4].

A review of various research on the mathematical models of the hydrodynamic and thermodynamic nature of the ejector is provided in [5]. The thermodynamic model of the ejector is developed based on balance equations of mass, momentum and energy with specific interpretations for the ejector or its sections. According to review [5] in the majority of cases the flows inside the ejector can be treated as steady and one-dimensional. The friction of flows and non-ideal mixing leads to a non-isentropic process, which is evaluated by isentropic efficiencies in the nozzle, mixing and diffuser sections [1] and [6].

Compression efficiency of the ejector [5] and [7] is evaluated in terms of the energy recovered by the secondary flow with respect to the energy available in the primary flow. Above mentioned ejectors' models [5], characteristics of their properties [1] and [8] are widely validated experimentally or tested in practice.

As it was mentioned and shown above (Fig. 1 (c)), turbofan has turbine and fan located on common axis. There are application examples, when renewable energy driven wind turbine is employed to rotate fans to ventilate road tunnels [9]. This type of turbofan is often applied in industry [10] when burning natural gas.

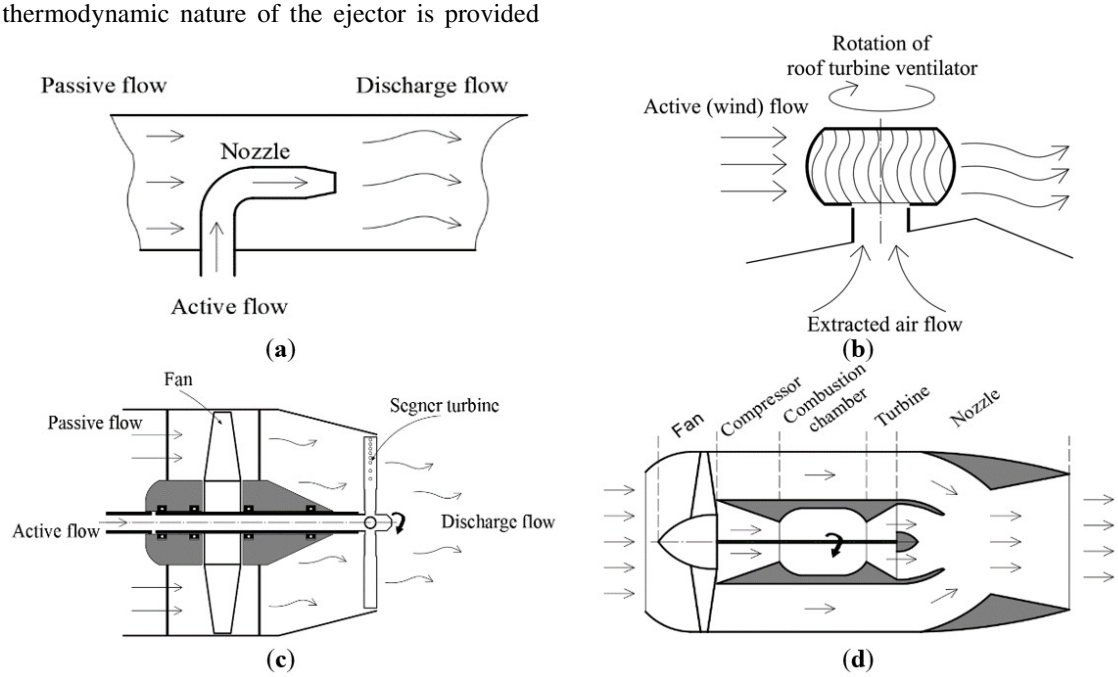

Fig. 1. *Devices, the functionality of which is obtained by using the potential and kinetic energy of flows by mixing them: a) ejector; b) roof turbine ventilator; c) turbofan – gas mixer; d) turbofan – engine*

When discussing the turbofans, one should keep in mind the peculiarities of microturbines [11]. These devices discover their application area from dental medicine [12] to the small-scale energy systems [13] or other micro systems [14]. In the context of the analysis presented here, it is important that the performance indicators of microturbines differ significantly from traditional energy turbines [15].

There are dozens of patents, the majority of cases of which involve gas burners [16] and [17]. Unfortunately, scientific papers rarely focus on such specifics, to the best of authors' knowledge there are no thermodynamic models, describing their operation in a similar way as ejectors are described. This hinders the preliminary assessment of their applicability.

The distinctive characteristics of turbofans as well as the nature of their variation may correspond to the specific application areas of the technological equipment (e.g. ventilation, air conditioning, refrigeration), which require certain flow mixing parameters. This may be relatively new areas, such as personalized ventilation [18], compressed air energy storage [19], integration in road tunnel ventilation [9] and [20]. When considering the potential application of a turbofan, preliminary indications about the basic characteristics, such as efficiency of compression and entrainment ratios, are required. For these applications, supersonic flow is not typical, so the methodology developed below in the paper is limited to the analysis of subsonic modes.

So far there is a gap in knowledge in which case the turbofan or ejector is superior or inferior to each other. The goal of this paper is to compare thermodynamic processes in the ejector and the turbofan when they have the same initial states of active and passive flows. The path to obtain turbofan's characteristics based on the adapted thermodynamic model of ejector was chosen. The proposed model is compared to well known, broad-mode and fluid range validated ejector thermodynamic model. The latter has been modified and detailed here to allow symmetric comparison of ejector and turbofan thermodynamic models. Here, it is very important to determine the internal irreversibility (loss) of the processes.

Quantitative indicators, required to solve the tasks are defined using analytical, empirical, and numerical models as well as combination of their equations. The presented preliminary comparison of performance thermodynamic models for the mentioned devices, so far was not described in the literature. The article would claim to be considered as theoretical or conceptual one. The analytical equations of flow processes and their interpretations found in the textbooks of engineering thermodynamics are chosen for this case and prevail in the article. The authors believe that using/selecting five process irreversibility coefficients for the estimated entropy enabled to minimize the empiricism, common in technology sciences.

The article is structured as follows: Section 1 explains ideal processes in ejector and turbofan. Section 2 describes in detail the adapted thermodynamic model of the process in the ejector. Section 3 presents the thermodynamic model of the turbofan in parallel with the main accents of ejector model. The assessment and comparison of the main performance indicators (compression and entrainment ratios as the resulting comparative parameters) of both devices for the case study are presented in Section 4. The conclusions are summarized in Section 5.

1 IDEAL PROCESSES IN THE EJECTOR AND TURBOFAN

Simplified schemes of the compared devices with their characteristic parameters are presented: ejector – Fig. 2 and turbofan – Fig. 3. The main components of the ejector depicted in Fig. 2 are: nozzle, mixing chamber and diffuser. The main components of the turbofan (Fig. 3) are the air turbine and fan.

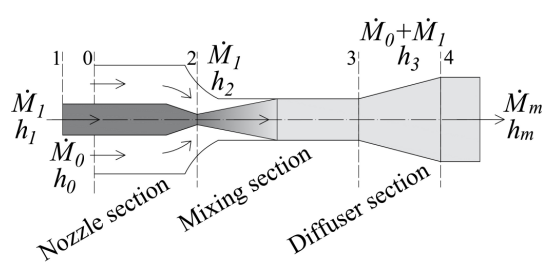

Fig. 2. *Simplified scheme of the ejector (the numbers next to the cross-sections correspond with the indices used in equations and diagrams*

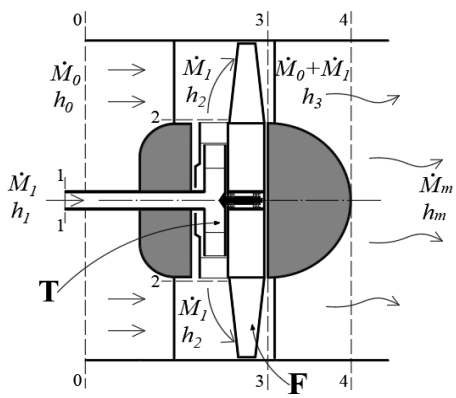

Fig. 3. *Simplified scheme of the turbofan: T – turbine, F – fan*

The purpose of these devices is to create a mixture that has the required flows mass ratio $\bar{M} = \dot{M}_0 / \dot{M}_1$ and to provide this mixture with pressure P_m. In both devices, the passive flow of enthalpy h_0 (or pressure P_0) is induced by the active flow expressed as enthalpy h_1 (or pressure P_1). These flows are mixed and mixture attains the state of enthalpy h_m (or pressure P_m). The following relationship exists between the states that define these processes:

$$P_0 < P_m < P_1 \quad \text{or} \quad h_0 < h_m < h_1 \tag{1}$$

Above mentioned common states for both devices and related ideal gas processes are shown in *h–s* diagram (Fig. 4). At first let us consider these processes to be ideal, when internal irreversibility in each section is expressed by $\Delta S_{ir} = 0$ and let us denote states that correspond with that with the ' index.

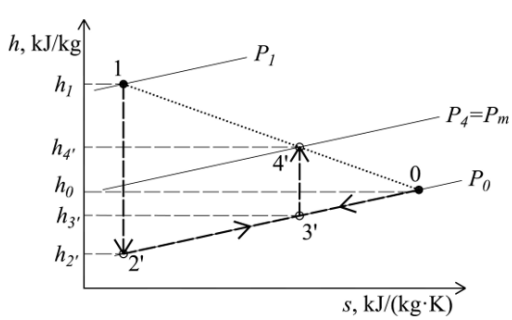

Fig. 4. *Ideal mixing processes in ejector and turbofan*

In an ideal case, initial state of active flow is marked as state 1 and for a passive flow – 0. For the ideal processes, initial state of the mixture (3') is on the P_0 isobar that connects states 0 and 2'. Finally, resulting state of the mixture is state 4', which is on the line that connects states 0 and 1. The ratio of ideal compression and ideal expansion $\left(h_{4'} - h_{3'}\right) / \left(h_1 - h_{2'}\right)$ is considered to be an indicator of the identity of the initial conditions of both devices.

The first law of thermodynamics (FLT) and the second law of thermodynamics (SLT) in this case are expressed as follows:

$$\dot{M}_{1'}^{+} h_1 + \dot{M}_0^{+} h_0 = \left(\dot{M}_{1'}^{-} + \dot{M}_0^{-}\right) h_{4'}, \tag{2}$$

$$\dot{M}_{1'}^{+} s_1 + \dot{M}_0^{+} s_0 = \left(\dot{M}_{1'}^{-} + \dot{M}_0^{-}\right) s_{4'}. \tag{3}$$

The parametric equation resulting from the FLT and SLT enables to determine the specific location of point 4' for the enthalpy and entropy of this mixture:

$$s_{4'} = \frac{\dot{M}_{1'} s_1 + \dot{M}_0 s_0}{\dot{M}_{1'} + \dot{M}_0} \text{ and } h_{4'} = \frac{\dot{M}_{1'} h_1 + \dot{M}_0 h_0}{\dot{M}_{1'} + \dot{M}_0}. \tag{4}$$

One of the most important indicators of such a process is the ratio between the flow mass rates– entrainment ratio $\bar{M}_{'}$:

$$\bar{M}_{'} = \frac{\dot{M}_0}{\dot{M}_{1'}} = \frac{h_1 - h_{4'}}{h_{4'} - h_0} = \frac{s_1 - s_{4'}}{s_{4'} - s_0} \tag{5}$$

The location of point 4' on the diagram allows determining the pressure P_m of the mixture in the idealized process.

Another important performance indicator would be efficiency of compression, which demonstrates the ratio of the achieved result and the accompanying costs:

$$\eta_m = \left(\dot{M}_{1'} + \dot{M}_0\right)\left(h_{4'} - h_{3'}\right) / \dot{M}_{1'}\left(h_1 - h_{2'}\right) \tag{6a}$$

or

$$\eta_m = \left(1 + \bar{M}_{'}\right) \frac{\left(h_{4'} - h_{3'}\right)}{\left(h_1 - h_{2'}\right)}. \tag{6b}$$

These two indicators together characterize the performance of the device. They must be defined for actual processes, i.e. evaluate the irreversibility of all processes in the devices.

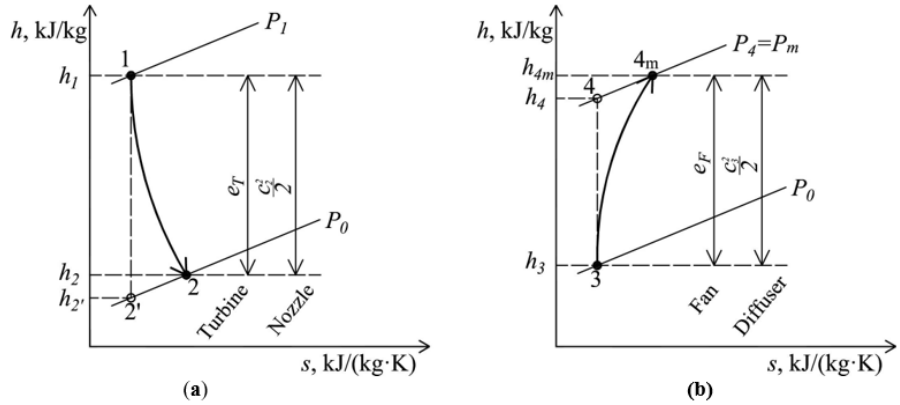

Fig. 5. *Energy conversion processes on the h-s diagram in the components of the ejector and the turbofan: a) the turbine (T) and the nozzle; b) the compressor or the fan (F) and the diffuser*

Ideal expansion 1-2' and compression 3'-4' and relevant actual processes 1-2 and 3-4m for both devices are drawn analogously, as shown in Fig. 5.

Thus, from a graphical point of view, i.e. from the first approach, the processes do not differ in these devices. Both in the nozzle of the ejector and the turbine of the turbofan the conversion of the state of the active component (that has a higher total energy or enthalpy) to another state takes place. However, there is a difference. Transformations linked to kinetic energy take place in the ejector. In the nozzle of the ejector a flow process takes place, i.e. the energy of the active component is converted to flow velocity C_2 (kinetic energy of the flow $C_2^2/2$). The energy form obtained in the turbine is expressed specific mechanical work of the turbine e_T. Analogously, only opposite processes occur in the diffuser and the fan. Actual processes properties depend both on the above mentioned inherent differences of the processes, as well as on specific irreversibility properties of their specific components. This will be discussed further, where thermodynamic models for each device will be presented.

The processes in this paper are limited to cases when both fluids are of the same nature, incompressible and the flow is subsonic. This limitation has no significant effect on the planned essential assessments of the thermodynamic analysis of devices (balance equations and graphical representation) as well as the comparison of processes that take place therein and the efficiency thereof.

The thermodynamic statement, when and how much the device with the energy transformation through mechanical work is more efficient than another device, in which the kinetic energy is directly transferred between the two streams, is the interest of this work. This statement will be proven on the basis of equivalent thermodynamic models for both devices. Proposition of such balanced minuteness models is important part of the study presented.

2 THE THERMODYNAMIC MODEL OF THE PROCESS IN THE EJECTOR

This work compares and discusses the thermodynamic models of two devices – ejector and turbofan – designed to prepare a mixture of the selected mass ratio and state for the two ideal gas subsonic flows. We start with the ejector as a widely-known yet specific device used for flow mixing. Its specific feature is that the energy of the active flow (the flow that has a higher total enthalpy) is used to entrain the passive flow (the flow that has a lower total enthalpy) and to provide the mixture thereof with the momentum that is required in order to create the potential and kinetic energy of that mixture and to transport that mixture between the devices in the system.

The structure of thermodynamic ejectors' models designed to assess the processes that take place already exists and related cases have been presented in the introduction. The model is based

on balance equations of mass, momentum and energy for the ejector or its sections. In the majority of cases the flows inside the ejector can be treated as steady and one-dimensional.

The specifics of each model usually reflect the objectives and specifics of this paper. The usual sequence is followed in this paper. In order to correctly compare the ejector and turbofan, certain adjustments have been made.

In order to compare actual and idealized processes they are drawn on the same *h-s* diagram (Fig. 6). Dry air when subsonic flow is present has been selected for the case study. Influence of air humidity is not investigated as it is negligible at the context of this research. The initial state is 1 (1.9 bar) for the active flow and 0 (1.01325 bar) for the passive flow. The same pressure P_m is to be obtained in the actual process. For this, the mass flow rate from idealized to actual processes should be increased $\dot{M}_1 > \dot{M}_{1'}$. In addition, the state of the resulting mixture in this case on this P_m isobar would shift to the right from point 4' to 4_m. We will discuss this transformation step-by-step.

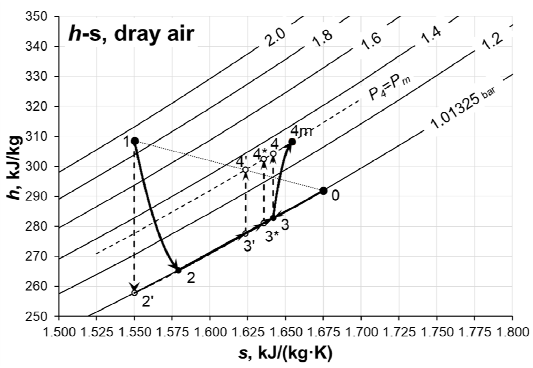

Fig. 6. *The depiction of the analyzed processes in the ejector on the h-s diagram*

In the actual process, the active flow that flows out of the nozzle expands until it reaches pressure P_0, state 2 and velocity C_2, which is expressed as follows:

$$C_2 = \sqrt{2\left(h_1 - h_2\right)} = \sqrt{2\left(h_1 - h_{2'}\right)\eta_{Ns}}\,, \qquad (7)$$

where $\eta_{Ns} = \dfrac{\left(h_1 - h_2\right)}{\left(h_1 - h_{2'}\right)}$ – the isentropic efficiency of nozzles (see the *h-s* diagram).

Having thus evaluated the internal irreversibility of the flow in the nozzle, the state of the mixture before the diffuser on the h-s diagram will shift from point 3' to the right $\Delta s_N = \Delta s_{3'-3*}$ to point 3*. Then, after the ideal diffuser we would have the equivalent of point 3* – point 4* on the pressure line P_m. If we consider the velocity equalizing process of both components in the mixing section as isobaric, $P_2 = P_3 = P_0$, we can assess the internal irreversibility of this process in terms of the produced entropy $\Delta s_M = \Delta s_{3*-3}$. We have the corresponding enthalpy h_3 and the isentropic efficiency of mixing chamber η_{Ms}. The authors propose to express this efficiency, using the process parameters depicted on the *h-s* diagram, as follows:

$$\eta_{Ms} = \frac{\left(h_2 - h_{3*}\right)}{\left(h_2 - h_3\right)}\,, \qquad (8)$$

and after the ideal diffuser point 4 on the pressure line P_m would be obtained.

When transitioning to the actual diffuser, it is necessary for the velocity C_3 at the rear of the mixing chamber (i.e. before the diffuser) to become $C_4 \approx 0$ once the flow reaches the rear of that diffuser on cross-section 4, and that its pressure and enthalpy remain P_m and h_{4m}, respectively. Having linked this to the actual process in the diffuser:

$$C_3 = \sqrt{2\left(h_{4m} - h_3\right)} = \sqrt{2\frac{\left(h_4 - h_3\right)}{\eta_{Ds}}} = \sqrt{2\frac{\left(h_{4'} - h_{3'}\right)}{\eta_{Ds}}}\,, \qquad (9)$$

where $\eta_{Ds} = \dfrac{\left(h_4 - h_3\right)}{\left(h_{4m} - h_3\right)} = \dfrac{\left(h_{4'} - h_{3'}\right)}{\left(h_{4m} - h_3\right)}$ is the isentropic efficiency of the diffuser. In Eq. (9) and the expression of η_{Ds} the enthalpy difference was changed in accordance with the equation observed in the process on the *h-s* diagram, $h_4 - h_3 = h_{4*} - h_{3*} = h_{4'} - h_{3'}$, because isobars P_m and P_0 are almost parallel and the distance in the direction of *s* in terms of the entire diagram is small.

Velocities C_0, C_2 and C_3 are related by the process in the mixing chamber which is denoted by a dashed line in Fig. 2. In quantitative terms, it is defined by the momentum equation using these velocities and corresponding cross-sections:

$$\begin{aligned} &P_2A_2 + P_0A_0 + \dot{M}_1C_2 + \dot{M}_0C_0 = \\ &= P_3A_3 + \left(\dot{M}_0 + \dot{M}_1\right)C_3 + F_{2-3} \end{aligned}, \qquad (10)$$

where F_{2-3} is the force between cross-sections 2 and 3.

When analysing ejectors, it is assumed that the mixing process takes place at a constant pressure $P_2 = P_3 = P_0$, areas of cross-sections are linked $A_2 + A_0 = A_3$, $F_{2-3} = 0$ and $C_0 = 0$. In order to assess these assumptions in quantitative terms, in this paper we propose using the isentropic efficiency of mixing chamber and the corresponding produced entropy. Therefore the momentum Eq. (10) can be expressed as $\dot{M}_1C_2\sqrt{\eta_{Ms}} = \left(\dot{M}_0 + \dot{M}_1\right)C_3$ and readjusted as follows:

$$\frac{\dot{M}_0}{\dot{M}_1} = \sqrt{\eta_{Ms}}\,\frac{C_2}{C_3} - 1 \text{ or } \bar{M} = \sqrt{\eta_{Ms}}\,\frac{C_2}{C_3} - 1, \qquad (11)$$

Having used Eq. (7) and Eq. (9), as actual processes take place in the ejector, it follows that:

$$\bar{M} = \frac{\dot{M}_0}{\dot{M}_1} = \sqrt{\eta_{Ns}\eta_{Ms}\eta_{Ds}\,\frac{\left(h_1 - h_{2'}\right)}{\left(h_{4'} - h_{3'}\right)}} - 1, \qquad (12)$$

Using this equation we can find the actual flow rate of the active fluid $\dot{M}_1$ under actual conditions of the process efficiency, evaluated by $\eta_{Ns}, \eta_{Ms}, \eta_{Ds}$. The initial state of the active flow, according to the *h-s* diagram, is 1 and the initial state of the passive flow (flow to be transported) is 0 and its mass flow rate $\dot{M}_0$. When analyzing the *h-s* diagram these initial conditions can be expressed as follows:

$$\begin{aligned} &\frac{h_{4'} - h_0}{h_1 - h_0} = \frac{h_{4'} - h_{3'}}{h_1 - h_{2'}} = \frac{1}{1 + \bar{M}_{'}} \quad \text{or} \\ &\bar{M}_{'} = \frac{h_1 - h_0}{h_{4'} - h_0} - 1 \end{aligned}, \qquad (13)$$

and then the equation that expresses the relationship between the main indicators of the actual and ideal ejectors – the entrainment ratio and coefficients of isentropic efficiencies of processes, is valid:

$$\bar{M} = \sqrt{\eta_{Ns}\eta_{Ms}\eta_{Ds}\left(1 + \bar{M}_{'}\right)} - 1. \qquad (14)$$

3 THE PROCESS IN THE TURBOFAN ALONGSIDE THE PROCESS IN THE EJECTOR

In the nozzle of the ejector a flow process takes place with energy losses, evaluated as the isentropic efficiency of the nozzle η_{Ns}. In this case there is no mechanical work. A work process takes place in the turbine, with corresponding energy losses, evaluated as the isentropic efficiency of the turbine $\eta_T = \left(h_1 - h_2\right) / \left(h_1 - h_{2'}\right)$. Even though this expression is analogous to η_{Ns}, their numeric values differ due to different $\Delta s_{2-2'}$ which depends on the distinctive properties of the component (turbine or nozzle).

When presenting the processes in the turbofan below, the device will be compared with the process in the ejector which was discussed in chapter 2. The work obtained in the turbine and the momentum obtained in the nozzle are used in the next elements of the corresponding device. We have chosen the aggregation of most common losses which occur in the turbofan. As a result, we used "isentropic efficiency of the turbine" and "isentropic efficiency of the fan". It is hardly possible to estimate all losses that occur in practice. In our research, these efficiencies are accepted on the basis of engineering practice and published investigations, the losses in microturbines are analyzed widely in [12], [13], [15] and [16].

The specific mechanical work of the turbine is e_T or power $\dot{E}_T = e_T\dot{M}_1$ while the internal irreversibility of this process is evaluated as the isentropic efficiency of the turbine η_T. This power is transmitted to the fan installed on the same shaft without any energy losses. As in any fan, the change of state of the flow that is being mixed $\dot{M}_1 + \dot{M}_0$ takes place here which evidences itself as an increase of enthalpy. The

internal irreversibility of this process, including mixing and the restoration of pressure in the diffuser that is assigned to the fan, is evaluated as the isentropic efficiency of the fan η_F. In a more detailed analysis it can be divided to impeller, mixing and diffuser losses $\eta_F = \eta_{FI}\eta_{FM}\eta_{FD}$.

In quantitative terms, the process in the turbofan is expressed using the mechanical work of components which is expressed by the power balance equation:

$$e_T\dot{M}_1 = e_F\left(\dot{M}_1 + \dot{M}_0\right). \quad (15)$$

Both compression processes on *h-s* diagrams (Fig. 5 and Fig. 7) are depicted using process lines with the same indices. Fig. 7 is a simplified version of Fig. 6. The main processes on the *h-s* diagram for the ejector (EJ) and the turbofan (TF) are depicted in an analogous manner.

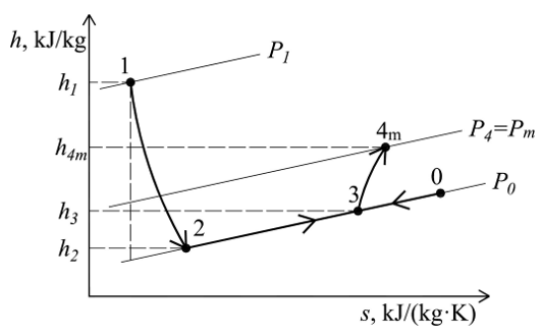

Fig. 7. *The processes of the change of state of components that are being mixed in the EJ and the TF*

Eqs. (11) and (15) serve as the basis of the dependence on the entrainment ratio for each of the compared devices:

$$\bar{M}_{EJ} = \frac{C_2}{C_3} - 1 \quad (16a) \quad \text{and} \quad \bar{M}_{TF} = \frac{e_T}{e_F} - 1. \quad (16b)$$

In general, the velocity of the flow that leaves the nozzle at the defined difference of enthalpies and the isentropic efficiency of the nozzle (the ratio of the difference of actual and isentropic kinetic energies) η_{Ns} is expressed as follows:

$$C = \sqrt{2(h_1 - h_{2'})\eta_{Ns}}. \quad (17)$$

The specific work in the turbine is calculated likewise:

$$e = (h_1 - h_{2'})\eta_T. \quad (18)$$

Then Eqs. (16a) and (16b) can be rewritten as:

$$\bar{M}_{EJ} = \sqrt{\eta_{Ns}\eta_{Ms}\eta_{Ds}\frac{\left(h_1 - h_{2'}\right)}{\left(h_{4'} - h_{3'}\right)}} - 1, \quad (19a)$$

and

$$\bar{M}_{TF} = \eta_T\eta_{FI}\eta_{FM}\eta_{FD}\frac{\left(h_1 - h_{2'}\right)}{\left(h_{4'} - h_{3'}\right)} - 1. \quad (19b)$$

The efficiency of compression, based on Eq. (6) for actual process:

$$\eta_m = \left(M_1 + M_0\right)\left(h_4 - h_3\right) / M_1\left(h_1 - h_{2'}\right), \quad (20a)$$

or

$$\eta_m = \left(1 + \bar{M}\right)\frac{\left(h_4 - h_3\right)}{\left(h_1 - h_{2'}\right)} \approx \approx \left(1 + \bar{M}\right)\frac{\left(h_{4'} - h_{3'}\right)}{\left(h_1 - h_{2'}\right)}. \quad (20b)$$

The enthalpy difference could be changed in accordance with the equation observed in the process on the h-s diagram, $h_4 - h_3 = h_{4'} - h_{3'}$, because isobars P_m and P_0 are almost parallel and the distance in the direction of *s* in terms of the entire diagram is small.

On the basis of Eq. (19) and Eq. (20) the expressions of the efficiency of the EJ and TF are obtained:

$$\eta_{EJ} = \sqrt{\eta_{Ns}\eta_{Ms}\eta_{Ds}\frac{\left(h_1 - h_{2'}\right)}{\left(h_{4'} - h_{3'}\right)}} \cdot \frac{\left(h_4 - h_3\right)}{\left(h_1 - h_{2'}\right)}, \quad (21a)$$

and

$$\eta_{TF} = \eta_T\eta_{FI}\eta_{FM}\eta_{FD}\frac{\left(h_1 - h_{2'}\right)}{\left(h_{4'} - h_{3'}\right)} \cdot \frac{\left(h_4 - h_3\right)}{\left(h_1 - h_{2'}\right)}. \quad (21b)$$

Having applied the previous assumption that $h_{4*} - h_{3*} = h_4 - h_3 = h_{4'} - h_{3'}$:

$$\eta_{EJ} = \sqrt{\eta_{Ns}\eta_{Ms}\eta_{Ds}\frac{(h_{4'}-h_{3'})}{(h_1-h_{2'})}}\,, \qquad (22a)$$

and

$$\eta_{TF} = \eta_T\eta_{FI}\eta_{FM}\eta_{FD}\frac{(h_1-h_{2'})}{(h_{4'}-h_{3'})}\cdot\frac{(h_4-h_3)}{(h_1-h_{2'})}\,. \qquad (22b)$$

When comparing the efficiencies of these two devices it follows that:

$$\frac{\eta_{TF}}{\eta_{EJ}} = \frac{\eta_T\eta_{FI}\eta_{FM}\eta_{FD}}{\sqrt{\eta_{Ns}\eta_{Ms}\eta_{Ds}\frac{(h_{4'}-h_{3'})}{(h_1-h_{2'})}}}\,, \qquad (23)$$

and the entrainment ratio proportion thereof, with the same main starting thermodynamic parameters $(h_1-h_{2'})/(h_{4'}-h_{3'})$:

$$\frac{\bar{M}_{TF}}{\bar{M}_{EJ}} = \frac{\eta_T\eta_{FI}\eta_{FM}\eta_{FD}\frac{(h_1-h_{2'})}{(h_{4'}-h_{3'})}-1}{\sqrt{\eta_{Ns}\eta_{Ms}\eta_{Ds}\frac{(h_1-h_{2'})}{(h_{4'}-h_{3'})}-1}}\,. \qquad (24)$$

4 REZULTS OF THE THERMODYNAMIC ANALYSIS

4.1 Processes that The Place in the Ejector

The numeric analysis of the presented model under the initial conditions listed in Table 1 (dry air and subsonic flow) is presented below.

Table 1. *Initial air state parameters for the numerical examples*

	Initial state parameters, data for all analysed cases		
	h, kJ/kg	*s*, kJ/kgK	*P*, Pa
1	308.6	1.55	190000
0	292.0	1.675	101325
2'	257.8	1.55	101325

The *h-s* diagram in Fig. 8 and Table 2 present the results of three numeric examples of the analytical explanation provided above. These cases correspond with the structure of the detailed diagram depicted in Fig. 6, where the numeric case of $M_0/M_{1'}$ = 1.33 is shown. For the purpose of an equivalent comparison of the essential results, identical isentropic efficiencies $\eta_{Ns}, \eta_{Ms}, \eta_{Ds}$ were selected for all cases (0.85; 0.90; 0.85, respectively [9]).

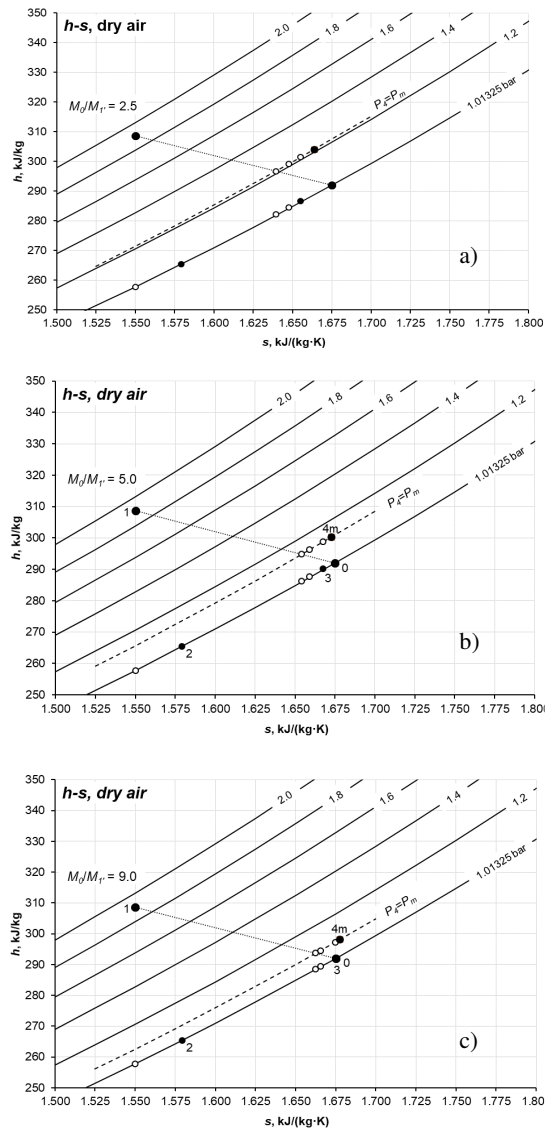

Fig. 8. *The depiction of numeric examples of the process in the ejector on the h-s diagram: a) when M_0/M_1= 2.5; b) when M_0/M_1= 5; c) when M_0/M_1= 9. Other data corresponds with Tables 1 and 2*

Table 2. *The results for three cases when subsonic flows of air are mixed in the ejector*

	Numeric cases in accordance with Eq. (18)								
	$M_0/M_{1'}$=2.5			$M_0/M_{1'}$=5			$M_0/M_{1'}$=9		
	η_{Ns}	η_{Ms}	η_{Ds}	η_{Ns}	η_{Ms}	η_{Ds}	η_{Ns}	η_{Ms}	η_{Ds}
	0.85	0.9	0.85	0.85	0.9	0.85	0.85	0.9	0.85
	State parameters typical of the process								
	h, kJ/kg	s, kJ/kgK	P, Pa	h, kJ/kg	s, kJ/kgK	P, Pa	h, kJ/kg	s, kJ/kgK	P, Pa
2	265.4	1.579	101325	265.4	1.570	101325	265.4	1.579	101325
3'	282.2	1.639	101325	286.3	1.654	101325	288.6	1.663	101325
4'	296.8	1.639	121331	294.8	1.654	113029	293.7	1.663	108696
3*	284.6	1.648	101325	287.7	1.659	101325	289.4	1.665	101325
4*	299.2	1.648	121331	296.2	1.659	113029	294.5	1.665	108696
3	286.7	1.655	101325	290.2	1.668	101325	292.1	1.675	101325
4	301.5	1.655	121331	298.8	1.668	113029	297.2	1.675	108696
4_m	304.1	1.664	121331	300.3	1.673	113029	298.2	1.678	108696
	Main results								
	M_0/M_1	$M_1/M_{1'}$	η_m	M_0/M_1	$M_1/M_{1'}$	η_m	M_0/M_1	$M_1/M_{1'}$	η_m
	Eq. (12)	Eq. (13)/ Eq. (14)	Eq. (20)	Eq. (12)	Eq. (13)/ Eq. (14)	Eq. (20)	Eq. (12)	Eq. (13)/ Eq. (14)	Eq. (20)
	0.509	4.916	0.438	0.975	5.128	0.334	1.550	5.806	0.258

In Figs. 5, 6, 7, 8 closed dots depict the states of the actual process while open dots are used in order to convey the concept of thermodynamic models (see Fig. 6).

It should once again be noted that this paper presents a case when the pressure P_m and mass flow rate $\dot{M}_0$ of the mixture obtained in the ideal process following the proportions of component should be preserved when transitioning to the actual process. For this purpose, the mass flow rate of the active fluid is increased in terms of the ideal case, $\dot{M}_1 > \dot{M}_{1'}$. As the $\dot{M}_0$ component relatively increases, P_m moves towards the pressure line of $\dot{M}_0$ (1.01325 bar).

The enthalpy of the mixture decreases while the entropy increases, in turn increasing the internal irreversibility of the process. The relationship between Eq. (13) and Eq. (14) shows that this mass flow rate has to be increased. Compared with the ideal process for each case, $M_0/M_{1'}$= 2.5; 5; 9, the mass flow rate of the active flow has to be increased almost five times while the efficiency of compression is nearly halved. This is depicted in Fig. 9.

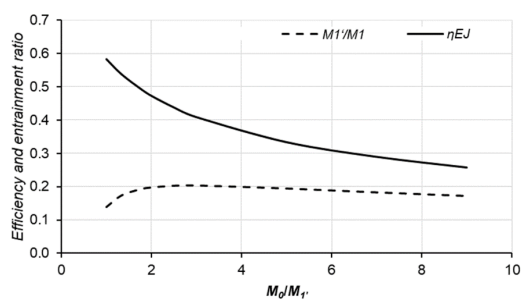

Fig. 9. *Variation in actual active mass flow rate and the efficiency of compression of the ejector subject to the selected mass flow ratio in the idealized process*

Other cases are possible, for example, the aim to preserve the initial ratio of mass flow rates $\bar{M}$ i.e. they should remain the same in both ideal and actual cases. Then the pressure of the mixture

would be lower than P_m, significantly reducing the efficiency. The results of the comparison of the turbofan and ejector are presented below.

4.2 Assessment of the Main Performance Indicators of the Ejector and the Turbofan

Fig. 10 shows the results of the comparison of the most important performance characteristics for the processes that take place in the ejector and turbofan, obtained using Eqs. (22) to (24). All those dimensionless or ratio-based characteristics are given depending on the already mentioned initial conditions $(h_{4'} - h_{3'})/(h_1 - h_{2'})$. These conditions are unambiguously related to the entrainment ratio of the ideal ejector, expressed by Eq. (13) or (5). Fig. 10 shows the numerical link between the following initial conditions and three cases of $M_0/M_{1'}$ (see Table 2) for the ejector: 2.5, 5.0 and 9.0.

The figure shows that according to the equations obtained during the analysis, the devices compared here have different sensitivity to the initial conditions. When both Eqs. (23) and (24) are equal to 1 (see also 1 in the ordinate axis), the performance indicators for the same initial flow conditions for both devices are the same. From here towards lower values of $(h_{4'} - h_{3'})/(h_1 - h_{2'})$ (on the left side of the diagram) the TF has an advantage over the EJ. As shown in the figure, the actual efficiency of compression of the ejector at that location is about 33% (Eq. 21a) and the entrainment ratio is almost 1 (Eq.19a).

The intersection of the indicators depicted on the diagram (colored dots) depends on the numeric values of the combination of isentropic efficiencies $\eta_T \eta_F$ and $\eta_{Ns}\eta_{Ms}\eta_{Ds}$. The above widely discussed they are assumed as (point and lines – green): $\eta_T = 0.5$; $\eta_{FI} = 0.8$; $\eta_{FM} = 0.9$; $\eta_{FD} = 0.9$. Thus, $\eta_F = 0.8 \times 0.9 \times 0.9 = 0.65$. For ejector – $\eta_{Ns} = 0.85$, $\eta_{Ms} = 0.90$, $\eta_{Ds} = 0.85$.

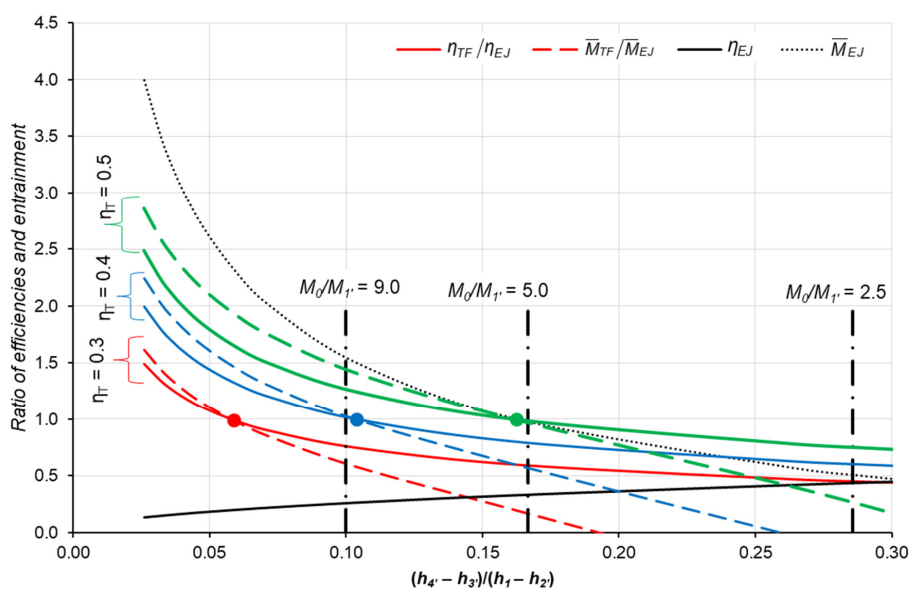

Fig. 10. *The comparison of the main performance indicators of the ejector and turbofan under the same starting conditions* $(h_{4'} - h_{3'})/(h_1 - h_{2'})$, *Eq. (13)*

This competitiveness boundary of the compared devices is determined analytically as $\left((\eta_T\eta_F)^2\right)/\left(\eta_{Ns}\eta_{Ms}\eta_{Ds}\right)$. This would be an indicator comparing the degree of irreversibility of the processes in these devices, for which no flow state parameters are required. In this case study it equals 0.16 from $((0.5 \times 0.65)^2/(0.85 \times 0.90 \times 0.85))$ while the corresponding $\dot{M}_0/\dot{M}_{1'}$ equals 5.07.

When we increase the isentropic efficiency of EJ components, we will have the case < 0.16 (the point of intersection of the comparative parameters will move to the left, see Fig. 10). When we increase the isentropic efficiency of microturbine or fan, we will have a case > 0.16.

These isentropic efficiencies are highly dependent on the size and other features of each evaluated component. While in a wide range $\eta_{Ns}\eta_{Ms}\eta_{Ds}$ are rather stable and well-researched, when it comes to small devices (micro-turbine with partial admission and micro-fan or micro-compressor) $\eta_T\eta_F$ can move quite away from 1.

This is demonstrated by additional sensitivity analysis by changing the efficiency of the microturbine. This is the parameter whose value has the least certainty at this stage of the research. The ejector's isentropic efficiencies are assumed as constant (see also Table 2) As already mentioned, in the case of Fig. 10 isentropic efficiency of microturbine is η_T = 0.5. In the case of η_T = 0.40 it is understood that the advantages of TF occur already at ejector entrainment ratio values higher than 1. These would be the cases to the left of $\bar{M}_{EJ} \approx 1.5$ (point and lines – blue). In the case of η_T = 0.30 of TF, the benefits appear for cases already to the left of $\bar{M}_{EJ} \approx 2.3$ (point and lines – red). The developed analytical model and this fragment of the sensitivity analysis show that in the design of TF, special attention must be paid at the microturbine's design.

The advantage of the TF over the EJ increases as the entrainment ratio on the basis of mass $\bar{M} = \dot{M}_0/\dot{M}_1$ increases. This means that based on the *h-s* diagram, when the initial and resulting state parameters are the same, the TF with the selected active flow rate will allow a higher amount of the passive flow to be pumped.

Due to the higher efficiency of compression and the accompanying entrainment ratios the TF could be relevant in terms of gas burners, roof turbofans and other specific devices. Natural gas burners that use full mixing require $\bar{M} \approx 18$. When entrainment ratios are low, the EJ has an advantage in terms of these indicators. The processes that take place in the TF and EJ are rather simplified in this paper. This allows authors to easily demonstrate or emphasize that in order to achieve higher entrainment ratios, converting the available energy to mechanical work enables the possibility of achieving better performance when compared with conversion to kinetic energy.

More thorough experimental research is required in order to determine the values of $\bar{M}$ and the absolute values of $\dot{M}_1$ and $\dot{M}_0$ at which it is efficient to use the TF. In addition to this, this device has moving parts, making its manufacturing process more complicated.

5 CONCLUSIONS

In the paper authors analysed the thermodynamic processes in the ejector and the turbofan when they have the same initial states of active and passive flows. This analysis is based on the parallel comparison of two thermodynamic models: one of them is created for turbofan and another one is adapted from the classical ejector. The characteristics, which demonstrate their efficiency – the efficiency of compression and entrainment ratios – were defined and compared at the subsonic flow mode conditions. The following conclusions were made:

1. The main cause of the resulting differences is the following. The mixing process in the ejector is realized via the interaction of kinetic energies that is expressed by the momentum balance equation. In the turbofan this occurs by transforming the energy of the active flow into the turbine work transferred to the fan, which conveys the passive flow. The process is defined by the work balance equations.
2. The case of numerical examples for the comparison of thermodynamic processes in the ejector and the turbofan when they have same initial states of active and passive flows $\left(h_{4'} - h_{3'}\right)/\left(h_1 - h_{2'}\right)$ shows that at lower values of these starting conditions (< 0.161) the TF

has an advantage over the EJ. The advantage of the TF over the EJ increases as the entrainment ratio on the basis of mass increases $\bar{M} = \dot{M}_0 / \dot{M}_1$. In this case the turbofan could be relevant in terms of gas burners, roof turbofans or other specific devices where a relatively higher passive flow rate is required.

3. The boundary between the advantage of the TF over the EJ on the basis of efficiency of compression and entrainment ratio indicators for the same initial flow conditions is determined analytically. These cases correspond to $\frac{(\eta_T \eta_F)^2}{\eta_{Ns} \eta_{Ms} \eta_{Ds}}$. It is 0.16 in the case of numerical examples and depends on the combination of isentropic efficiency of the components of both devices. In order to determine these specifics for the turbofan, a thorough experimental study is required, especially if a microturbine with partial admission is used.

The numerical results obtained comparing the models discussed in the paper are limited to air-to-air flows mixing at subsonic regime. Considering similarities to ejector, turbine and ventilator, presented thermodynamic model could serve as a basis for the creation of the theoretical model for roof turbine ventilators. The developed model could serve also as a basis for its development into supersonic analysis.

6 ACKNOWLEDGEMENTS

This project has received funding from European Regional Development Fund project No 01.2.2-LMT-K-718-01-0016 under grant agreement with the Research Council of Lithuania (LMTLT).

7 NOMENCLATURE

A	cross-section area, [m^2]
C	velocity, [m·s^{-1}]
$\dot{E}$	mechanical power, [kW]
e	specific mechanical work, [kJ·kg^{-1}]
F_{2-3}	power between cross-sections 2 and 3, [N]
h	enthalpy, [kJ·kg^{-1}]
$\dot{M}$	mass flow rate, [kg·s^{-1}]
$\bar{M}$	entrainment ratio (ratio of mass flow rates), [-]
P	pressure, Pa
S	entropy, [kJ·K^{-1}]
s	entropy, [kJ·kg^{-1} K^{-1}]
η	efficiency, [-]
η_{Ds}	the isentropic efficiency of diffuser, [-]
η_F	the isentropic efficiency of fan, [-]
η_{FD}	the efficiency of fan diffuser, [-]
η_{FI}	the efficiency of fan impeller, [-]
η_{FM}	the efficiency of mixing in fan, [-]
η_{Ms}	the isentropic efficiency of mixing chamber, [-]
η_{Ns}	the isentropic efficiency of nozzles, [-]
η_T	the isentropic efficiency of turbine, [-]

Superscripts

'	idealized state
+	in
–	out

Subscripts

0 to 4 air flow states at the cross-section (according to Fig. 2)

D	diffuser
EJ	ejector
F	fan
ir	irreversible
M	mixing chamber
m	mixture
N	nozzle
T	turbine
TF	turbofan

8 REFERENCES

[1] Ma, Z., Bao, H., Roskilly, A.P. (2017). Modélisation thermodynamique et détermination des paramètres de l'éjecteur pour des systèmes frigorifiques à éjection. *International Journal of Refrigeration*, vol. 75 , p. 117-128. DOI:10.1016/j.ijrefrig.2016.12.005.

[2] Ray, S.D., Glicksman, L.R. (2013) Increased Natural Ventilation Flow Rates through Ventilation Shafts. *International Journal of Ventilation*, vol. 12, p. 195-210. DOI: 10.1080/14733315.2013.11684016.

[3] Berisha, X., Meha, D. (2018). Modelling of direct connection of heat consumers to district heating with ejectors. *International Journal on Advanced Science, Engineering and Information Technology*, vol. 8, no. 1, p. 219-226. doi:10.18517/ijaseit.8.1.3246.

[4] Besagni, G., Mereu, R., Inzoli, F. (2016). Ejector refrigeration: A comprehensive review. *Renewable and Sustainable Energy Reviews*, vol. 52, p. 373-407. doi:10.1016/j.rser.2015.08.059.

[5] He, S., Li, Y., Wang, R.Z. (2009). Progress of mathematical modeling on ejectors. *Renewable and Sustainable Energy Reviews*, vol. 13, p. 1760-1780. DOI:10.1016/j.rser.2008.09.032.

[6] Antonio, Y.M., Périlhon, C., Descombes, G., Chacoux, C. (2012). Thermodynamic Modelling of an Ejector with Compressible Flow by a One-Dimensional Approach. *Entropy,* vol.14, p. 599-613. DOI:10.3390/e14040599.

[7] Banasiak, K., Palacz, H., Hafner, A., Buliński, Z., Smołka, J., Nowak, A.J., Fic, A. (2014). A CFD-based investigation of the energy performance of two-phase R744 ejectors to recover the expansion work in refrigeration systems: An irreversibility analysis. *International Journal of Refrigeration,* vol. 40, p. 328-337. DOI:10.1016/j.ijrefrig. 2013.12.002.

[8] Liu, F. (2014). Review on Ejector Efficiencies in Various Ejector Systems. In Proceedings of the *15th International Refrigeration and Air Conditioning Conference*; Purdue, 14-17 July, 2014; p. 1-10.

[9] Wang. Z., Wu, Y., Lu, S., Meng, X., Zhang, J. (2019). A study on model experiment and aerodynamic match of Wind Energy Fan (WEF). *Sustainable Cities and Society*, vol. 49 p. 101618. DOI:10.1016/j.scs.2019.101618.

[10] ГазТехСнаб», O. Turbojet gas burner (Горелка газовая турбореактивная)(in Russian) Available online: http://www.gaztehsnab.ru/products/gas-on-fire/gas-on-fire_13.html, accessed on 10 October 2019.

[11] Capata, R., Saracchini, M. (2018). Experimental campaign tests on ultra micro gas turbines, fuel supply comparison and optimization. *Energies*, vol. 11, p. 799. DOI:10.3390/en11040799.

[12] Juraeva, M., Park, B.H., Ryu, K.J., Song, D.J. (2017). Designing high-speed dental air-turbine handpiece by using a computational approach. *International Journal of Precision Engineering and Manufacturing*, vol. 18, p. 1403-1407. DOI:10.1007/s12541-017-0167-4.

[13] Khamis, A., Badarudin, Z.M., Ahmad, A., Rahman, A.A., Bakar, N.A. (2011). Development of mini scale compressed air energy storage system. *Proceedings of the 2011 IEEE 1st Conference on Clean Energy and Technology*, CET 2011, Kuala Lumpur, 27-29 June 2011, p. 151–156.

[14] Sun, S.C., Shi, G.C. (2011). Design, Simulation and Fabrication of an Air-Driven Microturbomachine. *Key Engineering Materials*, vol. 483, p. 611-615. DOI:10.4028/www.scientific. net/KEM.483.611

[15] Capata, R., Sciubba, E. (2015). Experimental fitting of the re-scaled Balje maps for low-reynolds radial turbomachinery. *Energies*, vol. 8, p. 7986-8000. DOI: 10.3390/en8087986.

[16] Adinskov. B.P. (1969). Turbo gas burner. Patent No. 262304 (USSR).

[17] Achmedov, P.B., Rashidov, F.K. (1970). Turbine gas burner. Patent No. 262304 (USSR).

[18] Dalewski, M., Melikov, A.K., Vesuly, M. (2014). Performance of ductless personalized ventilation in conjunction with displacement ventilation: Physical environment and human response. *Building and Environment*, vol. 81, p. 354-364. DOI: 10.1016/j.buildenv.2014.07.011.

[19] Tallini, A., Vallati, A., Cedola, L. (2015). Applications of micro-CAES systems: Energy and economic analysis. *Energy Procedia*, vol. 82, p. 797-804. DOI:10.1016/j.egypro.2015.11.815.

[20] Muhasilovic, M., Duhovnik, J. (2012). CFD-Based Investigation of the Response of Mechanical Ventilation in the Case of Tunnel-Fire. *Strojniški vestnik - Journal of Mechanical Engineering*, vol. 58, no 3, p. 183-190. DOI:10.5545/sv-jme.2009.091.